MEMS Fixtures for Handling and Assembly of Microparts

Isam N. Tahhan [1,*]   Yan Zhuang [2]   Karl F. Böhringer [1,‡]   Kris S. J. Pister [2,3]   Ken Goldberg [1]

University of California, Berkeley, CA 94720-1777
[1] Ind. Eng. and Op. Research   [2] El. Eng. and Computer Sciences   [3] Berkeley Sensor & Actuator Center

ABSTRACT

Fixtures are used to locate and hold parts during automated inspection, machining, or assembly. Microelectromechanical systems (MEMS) are tiny devices built in batch processes derived from integrated circuit fabrication. We describe a design for an array of **MEMS microfixtures** for parallel inspection, transport, and assembly of microfabricated parts.

In a microfixture array, parts are brought near the fixture by random motion provided e.g. by vibratory agitation. The fixture clamps actively close when the parts enter the fixture. In large future fixture arrays, electrostatic or optical sensors integrated into the fixture cell can trigger this clamping function. Each cell operates autonomously and no global control is necessary.

We fabricated a prototype cell consisting of two upfoldable fixture walls and a bimorph thermal actuator using a standard CMOS process. This approach allows batch fabrication of large numbers of cells on a single silicon wafer, as well as easy integration of sensors and actuators that autonomously close each cell when filled.

Keywords: MEMS fixtures, massively parallel assembly, micropart handling.

1. INTRODUCTION

The increasing miniaturization of high-volume consumer products such as disk drives, displays, and sensors calls for fundamental innovations in parts design and handling. Batch-fabricated micro-parts require the handling of greater numbers of smaller parts in a reduced amount of time. In addition, the limitations of silicon micromachining with its monolithic fabrication paradigm constitutes a problem for the design of more complex microsystems: combining microelectronics, micromechanics, and microoptics into a single fabrication process inevitably compromises all subsystems. Consequently, there has been a growing interest in new techniques for positioning, inspection, and assembly of parts at the micro scale [1]. These methods and tools should provide precise handling devices for fragile, microscopic parts and represent an interface to the 'macro-world.'

Fixtures are used in industrial parts handling and assembly. The approach given in this paper expands the fixture concept to the micro-scale, by using design and fabrication techniques based on microelectromechanical systems (MEMS) technology. Our goal is a microfixture that enables the handling of microscale pieces in a massively parallel way. The prototype device described in this paper is designed for surface-mount parts with dimensions 500 µm $\times$ 500 µm $\times$ 200 µm.

Conventional single micro-robot concepts use one or a few micromanipulator(s) that act on all parts sequentially, with the possible help of expensive computer vision (see e.g. [2,3]). The cell concept presented here can be integrated with a simple sensor that can be fabricated simultaneously with the mechanical structures by using a standard foundry CMOS process (see e.g. [4]).

The basic building block of such a device is the fixture cell, a cube-like structure of three walls, made of polysilicon and aluminum, located on a silicon substrate (wafer). **Figure 1** shows a 3D view of such a cell with the back and the side wall and the thermally driven actuator. Chamfers, flat 'guiding' structures with their outer corner curled-up, are located in front of the cell entrance, facilitating the entry of parts. The parts are randomly moved by random vibration that is induced to the cell (or cell array) by means of piezoelectric vibration [6].

---

[*] Current address: Bartels Mikrotechnik, Emil-Figge-Str. 76, D-44227 Dortmund, Germany;
Email: tahhan@robotics.eecs.berkeley.edu
[‡] Current address: University of Washington, Dept. of Electrical Engineering, 234 EE/CSE Bldg., Seattle, WA 98195-2500;
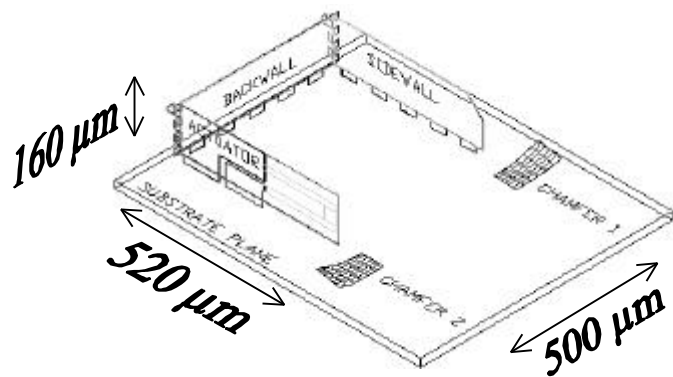Email: karl@ee.washington.edu

Figure 1. 3D view of upfolded fixture cell.

The principal idea is to obtain a *pallet for micro-parts.* Small parts can be cheaply batch-fabricated at high density, and subsequently handled, tested, and assembled at lower density. A somewhat similar approach has been used for macroscopic parts in the SONY APOS system [5]. APOS uses an array of nests (silhouette traps) cut into a vibrating plate. The nests are designed so that parts will remain in the nest only in one particular orientation. The nests eventually fill up when parts are flowing across the platform. We propose a similar approach at the micro scale and take advantage of micromachining processes to integrate sensors and actuators into the fixture cells.
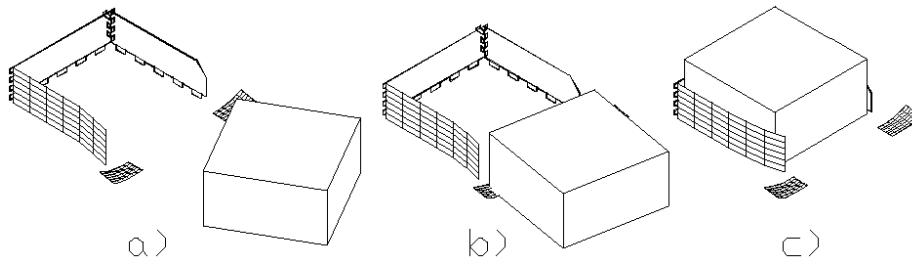

Figure 2 a-c. Schematic of part fixturing.

Figure 2 a-c depicts the capture of a part. At first, the part is located somewhere outside the cell (a). By random agitation, it eventually comes close to the cell entry, being guided by chamfers (b). As soon as the part is far enough inside, the sensor triggers closure of the cell, so that the part is held in place (c).

One wafer could carry very large numbers of fixture cells in rows and columns. The fixture array can be mounted on a piezoelectric vibratory platform [6] that provides random agitation of the parts. This allows massively parallel handling of the parts that will be fixtured, for example for inspection, transport, and assembly, by means of reusable and reliable micro tools.

Our concept combines the advantages of a single autonomous cell containing its own sensor with a batch fabrication process such as CMOS. For our prototype cell, the side walls were released in a simple back-end process using a XeF_2 gas phase etch [7]**.** Then the walls for the prototype had to be folded up and joined manually using a probe. The current design does not yet implement the sensor, since the emphasis for this prototype was on mechanical design issues.

In the next section we give an overview of related work concerning macro fixtures as well as MEMS techniques used, followed by a detailed description of both the mechanical cell features, and the estimated properties of the thermal actuator. Then, information on the postprocess release etch and assembly is provided. The paper is concluded by a description of results and future work, in particular the integration of the sensor and fabrication of multiple cells.

2. RELATED WORK

Fixtures are a widely used tool in industrial and automated manufacturing processes. A fixture is a device that locates and holds parts during assembly, inspection, or machining. It usually consists of a number of fixed locators and a flexible clamp [8]. Conventional fixtures are designed to hold a part in *form closure* [9]: the fixture geometry creates kinematic constraints

that prevent any infinitesimal motion of the part. In contrast, *force closure* [10] requires that the contacts be able to withstand any force or torque applied to the part.

For fixturing of micro parts we are interested in fixtures that provide force closure. The reason is that at micro scales, surface contact forces such as friction or stiction dominate other forces such as gravity or inertia (see e.g. [11]). However, for all calculations in this paper, only the conventional Coulomb friction model was used as a simple, conservative estimate.

Besides the difference in size by several orders of magnitude, the main innovation in our device is the idea of *active, independently actuated fixture cells*. Another difference between conventional (macro) fixtures and micro fixtures is the way parts are loaded into the fixture cell. In the latter, parts are often loaded from above, while we keep all motion except vibration in the substrate plane.

CMOS: One of the most common processes used in microelectronics is the CMOS (complementary metal-oxide-semiconductor) process, first introduced in the 1970's. Metal and oxide are the main materials used for a CMOS fabricated chip. Only a certain sequence of layers is available for building electrical as well as mechanical structures. Although many different variations of 'the' CMOS process are available nowadays, the basic sequence stays more or less the same. The current minimal linewidth lies below 0.5 µm, for electrical as well as (at least theoretically) mechanical features. For our device we used a standard foundry MOSIS-AMI 1.2µm CMOS process.[1]

MEMS: Microelectromechanical systems combine microelectronics and micromechanics. A multitude of MEMS devices have been developed, and several commercial products have appeared on the market (e.g., air bag sensors [12] and mirror array displays [13]).

CMOS for MEMS: The first work that showed the usage of CMOS for building mechanical structures was carried out in 1989 by Parameswaran et al. [14], building suspended beams and free standing bridges on a silicon wafer. Common examples of MEMS in CMOS are accelerometers with integrated electronics on one chip (e.g. [15]), integrated humidity sensors, and more.

A popular way to fabricate MEMS is to use standard processes (such as CMOS) with some additional post processing steps to create released mechanical components. Klaassen et al. [16], e.g., introduced the use of a bias voltage and a four electrode potentiostat to improve the selectivity of TMAH etchant, so that thermally isolated circuits could be fabricated.

Hinges and 3D MEMS: Another challenge in MEMS design is its intrinsically two-dimensional layout. A popular solution for building mechanical structures on a flat surface is to employ hinges for free standing structures. Hinges were described first in 1992 [17], and have proved since then to be a reliable tool to gain access to the 3rd dimension in MEMS. Hinges allow a rotation of released structures out of the wafer plane. An easy and elegant way of building these hinges in CMOS was established by Pister et al. [18], who used the aluminum layer to connect a suspended silicon beam to the substrate. The beam is entirely underetched in a post process step. Since aluminum is much more ductile and softer than polysilicon, the beam could be folded up by bending the metal hinges, leaving the silicon beam unbent. Furthermore, the stability of such hinges is enough to keep connected structures in place if they are not too heavy or strongly accelerated, taking advantage of the decreasing significance of mass and inertial effects with decreasing dimensions.

Thermal Actuators: Our miniature thermal actuator consists of a bimorph that is electrically heated. Power dissipates into heat in a polysilicon loop fabricated together with the actual bimorph. Due to different thermal expansion coefficients in the bi- or multimorph material, it is bent towards the side with the lower expansion coefficient. Excellent work in this area was done by Comtois et al. in 1995 [24], concerning theoretical as well as experimental aspects. They introduced the mathematical background so that detailed predictions could be made, covering the theoretical heating as well as resulting deflection of a multimorph actuator.

Advantages of thermal actuators are large deflection and / or high forces, ease of fabrication, and reliability. Disadvantages are the slower time constant (compared to other actuation principles) due to limited heat dissipation, and the rather high temperatures, as well as high energy consumption [23].

Thermal Actuators with Hinges: G. Lin [19] combined thermal actuators and hinges in her work on a heart cell muscle contraction sensor. The actuators have the function of cell resonators. Connected only by hinges to the substrate, they could be rotated out of the plane after a post-process release etch. The hinges served here as mechanical as well as electrical connections, since the actuator had to be driven by electrical power. Response time of the actuator in air was around 28 msec, and power consumption around 1.8 mA.

---

[1] The MOSIS Service, Information Sciences Institute, University of Southern California, 4676 Admiralty Way, Marina del Rey, CA 90292-6695, support@mosis.org.

3. MECHANICAL COMPONENTS

An important issue in designing MEMS is the dependency between desired functionality and fabrication process. In the macroscopic world, one can choose from a broad variety of materials, processes, and features; especially for prototyping. In the microscopic world, the range of materials is still very limited and depends on the particular process, so that they can not be seen as separate parameters. As a result, the achievable features strongly depend on the choice of the selected process. In other words, each process has its particular strengths and weaknesses for certain goals. In this paper, we want to show the advantageous use of the features provided by the standard CMOS process, while avoiding its drawbacks.

As shown in Fig.1, the fixture cell consists of four main entities: The sidewall, the backwall, the actuator, and the chamfers. Except the latter, all stuctures have to be folded up to form the cube-like cell body.

3.1. Walls

A problem when using a standard process is the limited range of materials available, as well as their fixed thickness when deposited on the substrate. **Table 1** gives an overview to all layers available in the process used (MOSIS-AMI 1.2μm).

Table 1. Layers available in CMOS process
(t = layer thickness; E = Young's Modulus;
α = thermal expansion coefficient).

Material	Shortcut	t [μm]	E [GPa]	α [10^{-6}/K]
Field Oxide	FOX	0.6	74	0.4
Polysilicon 1	POLY1	0.4	100	2.33
Oxide 0	OX0	0.075	74	0.4
Polysilicon 2	POLY2	0.4	100	2.33
Oxide 1	OX1	0.85	74	0.4
Metal 1	MTL1	0.85	69	23
Oxide 2	OX2	0.65	74	0.4
Metal 2	MTL2	1.15	69	23
Overglass	OG	1	-	-

Calculations were made to investigate if walls, consisting of certain combinations of layers, would withstand the forces that act on them during operation. Since the mass of a wall is small compared to the part to be fixtured, only the latter were taken into account. In preliminary experiments (see also [20]), 500 μm Si cubes ($\rho = 2.1$ gm/cm^3) were used on a piezoelectric vibratory platform with accelerations of up to 200 g (necessary to break surface stiction forces). For the acceleration force we get

$$F = m \cdot a = 515 \, mN. \tag{1}$$

The fixture wall dimensions were chosen as follows: wall height h = 160 μm, length l = 500 μm, with a strain limit $\varepsilon = 2 \cdot 10^{-3}$, and E = 69 GPa (both for aluminum). We are interested in the minimum required thickness for the fixture wall. The wall represents a cantilever beam that is bent around its base by a moment which equals M = F·h. By further using

$$I_Y = \frac{t^3 \cdot l}{12} \quad , \quad \boldsymbol{s} = \left(M \cdot \frac{t}{2}\right)/I_Y \quad , \quad \boldsymbol{s} = \boldsymbol{e} \cdot E \tag{2), (3), (4}$$

(I_Y = moment of inertia, referring to the bending axis along the wall length; t = wall thickness; σ = stress at the base; ε = strain; E = Young's Modulus),

we obtain for t_{min}

$$t_{min} = \sqrt{\frac{6 \cdot F \cdot h}{\boldsymbol{e} \cdot E \cdot l}} = 2.676 \, mm. \tag{5}$$

Thus the minimum wall thickness is approximately 2.7 µm. This result allows us to leave out the field oxide as well as the overglass layer, with the following advantage: It was observed that CMOS structures would curl out of the substrate plane much more when combined with either of these two layers [21]. It is presumed that the main reason for this behavior lies in the stress gradient between these layers. Field oxide (the first layer in the CMOS process) is thermally grown; hence it exhibits expansive stress when cooled down after deposition. On the other hand, the last layer, overglass, is spun on the wafer, so that it is under tensile stress when cured. Both forces together lead to the mentioned and observed curvature of a structure out of the plane. Consequently, the walls were designed to contain all layers except FOX and OG, leaving a theoretical thickness of 4.53 µm. (For further calculations, a practical thickness of 4.2 µm was used, in order to take certain losses due to overetch into account.) Note that in **Figure 8**, back– and side wall are illuminated evenly; indicating their flatness, whereas actuator and chamfers have dark corners (see discussions 'actuator' in Section 3.4 and 'chamfers' in Section 3.5, respectively).

3.2. Locks

Due to the potentially high accelerations acting on the cell generated by the vibratory platform and the freely moving parts, we have to ensure that the walls stay in the assembled position. A simple calculation shows that the hinges alone cannot prevent the walls from bending during operation.

Using the values from above, and $L = 160$ µm for the wall height, $L_h = 20$ µm for the hinge height alone, a wall thickness of $t_w = 4.13$ µm, a wall width $w_w = 500$ µm, a hinge width of 250 µm, and formula (2), we get for the deflection at the top of the wall y(x), according to [22]

$$y(x) = \frac{F}{E_2 \cdot I_2} \cdot \left(\frac{x^3}{6} - \frac{L}{2} \cdot x^2 \right) + \frac{F}{E_1 \cdot I_1} \cdot \left(\frac{L_h^2}{2} - L \cdot L_h \right) + \frac{F}{E_1 \cdot I_1} \cdot \left(\frac{L_h^3}{6} - \frac{L}{2} \cdot L_h^2 \right) \tag{6}$$

(F = force on beam end; I as in (2); index *1* for hinge, *2* for wall).

Comparing y(x = l) and L, we see that the resulting deflection is 21 % of the wall height – too much for a stable grip.

Therefore, we designed special support structures that keep sidewalls and backwall connected. These structures work partly as a zipper, partly as a hook. Once a wall is folded up, the overlapping corners fit into each other like a clasp. They then can be bent up to 90° to the back of the adjoining wall, so that they 'grasp' each other, providing a rather durable and easy-to-handle fixation. (Note that, for fixation, an angle of approx. 20° is already sufficient.)

Figure 3 shows such lock-edges on both sides of the depicted back wall. The material used for this ductile behavior is again aluminum; silicon alone would be too brittle and spring back or break.
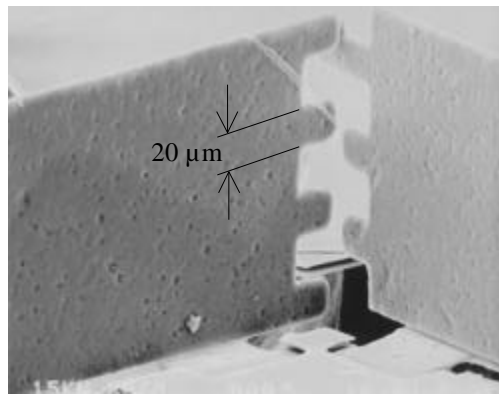

Figure 3. SEM picture of bent up back- and side wall, depicting the lock structures.

Another indication for structural improvements was the verification of resonance frequencies of the walls. Since stiffer walls have higher frequencies, f_{res} could be moved up from 16 kHz to 40 kHz. For a (rough) calculation, we used the model of a free standing wall (suspended beam model), and compared it to a wall that was additionally fixed on one edge (suspended triangle).

3.3. Hinges

To rotate the walls into the vertical position we employed aluminum hinges. **Figure 4** shows a simulated cross section of such a hinge. Two aluminum layers are stacked directly on top of each other, reaching both into the wall /actuator that has to be folded up (left), and onto the silicon substrate (right).
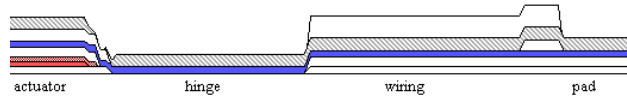

Figure 4. Simulated hinge cross section.

The hinge has to be underetched in order to fulfill its task; this is done simultaneously with the release etch of the walls. **Figure 5** shows a close-up view of such two hinges, before being bent into the vertical position. Note that the area between the hinges is darker than at their ends, since no reflecting silicon substrate is located beneath.

A drawback of aluminum hinges is that they will eventually break if bent up and down too often [22]. However, for the fixture cell a single out-of-plane rotation is sufficient.
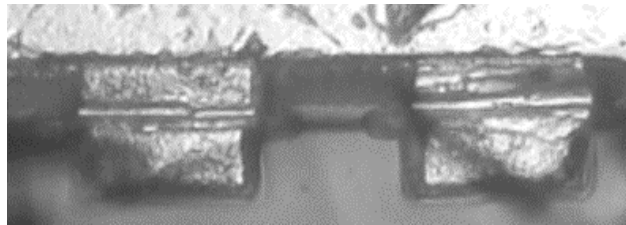

Figure 5. Close-up of underetched hinges.

Aluminum hinges simultaneously serve as mechanical, movable connections and as electrical connections, too. This feature was taken advantage of when designing the actuator.

3.4. Actuator

The actuator is one of the key component of the fixture cell. Since a CMOS process is used, certain actuation principles, such as electrostatic or magnetic ones, are ruled out or at least hard to realize. Thermal actuation was considered to be the most suiting principle, since rather high forces can be achieved [23], while the somewhat slow time constant was of no concern for the function of this device.

The actuator consists of two parts: a fixed portion that is connected to the substrate via metal hinges, and a moving portion with a built-in polysilicon loop. This loop is heated by electrical power, so that the actuator curls due to different expansion coefficients in its individual layers.

The static part is very similar to all other walls, although special care had to be taken to avoid shorting of the circuitry.

For the moving part, several parameters had to be taken into account: required force (to hold the part), best sequence of layers (for maximum range of motion / obtainable force), thickness (strength), and design of the polysilicon heater (electrical properties).

The force required to securely hold a part depends on the external forces and friction between cell and part. For a conservative estimate, we do not take further reduction by surface adhesion or possibly electrostatic forces into account. By using a safety factor of 5, we obtain an external (gravitational) force of 13 mN on a fixtured part (500 μm Si-cube). If we also take into account the angle of 45° under which the actuator hits the part, the following diagram shows the friction coefficient necessary:
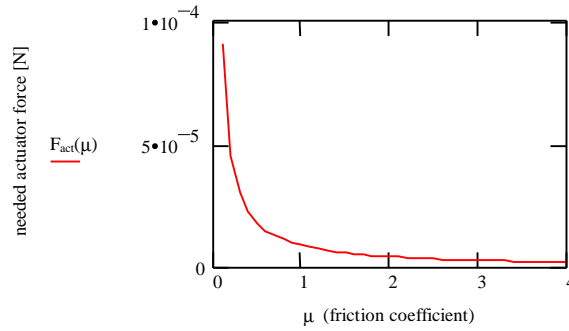
Figure 6. Friction coefficient and actuator force.

A friction coefficient μ of 1 or more is desirable in order to keep the necessary actuator force low. Since values for μ are possibly lower (0.1 and up, but no exact value for Si on Si microcontacts is available), it can be assumed that actuator force should be more than $5 \cdot 10^{-5}$ N.

Using the formulas from [24], we calculated the deflection of a bimorph actuator depending on the temperature rise and its sequence and thickness of layers. Since only the layer sequence can be varied in the standard CMOS process, different combinations were checked. After comparing the results to the minimally required thickness and deflection / force, a sequence of FOX - POLY1 - POLY2 - OX1 - MET1 - MET2 was considered to be the best compromise.
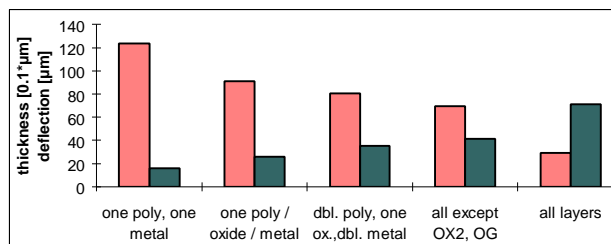

Figure 7. Theoretical deflection according to layers.

In this case, the expansive stresses of the FOX layer are wanted, in order to pre-curl the actuator towards the center of the cell. The purpose is that the actuator fixes the part in the 'cooled' position, using only spring forces, and that the cell is open when the actuator is heated. The advantage is that power can be shut off after fixturing and the cell can be used as a passive mechanical pallet. For release of the part, the cell can be heated with an external source (laser, heat gun, etc.) alternatively.

In the next step, the electrical properties were optimized by calculating the temperature rise at a power consumption of 50 mW, comparing different resistance quotients of poly and metal, so that most of the power would be dissipated in the heater, not in the wires. The layout of the heating loop was then adjusted to this value, which lies at around 550 Ω.

Table 2 shows the estimated properties of the actuator. (Due to fabrication flaws, leading to shorts in the circuitry, no experimental results could be gained; see 'shorts' in the last section.)

Table 2. Calculated properties of the thermal actuator.

Resulting temperature rise above ambient	$\Delta T = 228°K$
Estimated deflection	≈69 µm
Estimated force	ca. 880 µN at the zero position; ca. 440 µN after 50 % of max. deflection
Proportional factor	1.39 µm/mW or 17.553 µN/mW

3.5. Chamfers

The chamfers have the purpose to help parts find their way into the cell during random motion. In **Figure 8**, the two chamfers from above can be seen. It can be observed that one outer corner is bent up most (shown by the increasing darkness due to less reflected light), while the rest lies flat on the substrate. This effect is obtained by two means:

1. The curl comes from usage of all layers, including FOX and OG. As stated above, this leads to a clearly visible curvature out of the plane; the height verified under the microscope lies around 20 µm above the substrate surface.

2. The different curl distribution is achieved by corresponding, asymmetrical underetch, starting at just that corner.

4. FABRICATION AND POSTPROCESSING

The CMOS process brings together several advantages: It is widely available, well established, and it allows the easy integration of mechanical with electronic structures in one device, although certain restrictions for the mechanical part apply.

4.1. XeF$_2$-etch

CMOS as well as other processes used for MEMS, such as ORBIT, MUMPS / smartMUMPS, or iMEMS, usually require a postprocess release etch step. The objective is, among others, to allow safe transportation of the fabricated devices. In the case of CMOS, this was not originally intended, since the process was not developed for MEMS techniques. Nevertheless, mechanical structures in CMOS require being released from the substrate.

Two methods are commonly used for this purpose. The first one is to etch away one layer of the structure ('sacrificial' method). The second one etches away the silicon substrate. Silicon etchants can be anisotropic, like KOH, or isotropic, as XeF$_2$, or SF$_6$.

For the present case, XeF$_2$ [7] was being used, due to certain advantages: XeF$_2$ is a gas phase etchant so that no stiction problems arise. The process is also readily controllable. It can be observed by using a windowed etching chamber and a microscope. Eventually, the etch can be easily and quickly stopped by flooding the etching chamber with N$_2$. These features were exploited thoroughly for the release of the structures. The steps were performed as follows:

1. The holes at the upper edges of all walls had to be cleaned of remaining oxide and polysilicon that was not properly etched away during CMOS fabrication. For this purpose, buffered oxide etch (BOE) and hydrogen fluoride (HF) was used, depending on the severity of the contamination.

2. The sample was placed in the etching chamber, which was then evacuated and flooded with XeF$_2$. The etch can be visually monitored, and since the space between the hinges was designed to be transparent (only SiO$_2$ and OG), at the arrival of the etch front at the hinges, the etch was precisely stopped in order not to underetch the hinges too much. It could be observed that the front stayed quite parallel during its advance.

3. The chamber was flooded a few times with N$_2$ and evacuated before the sample could be taken out. Since no liquids were involved, the sample could be taken immediately to the probe station without any further treatment.

4.2. Assembly

A semi-automatic probe station was used to erect the walls and adjust the actuator position. The proceeding was as following:

(1) The back wall was erected under the microscope. Care had to be taken that it was pushed up uniformly to not overstress the wall surface. (2) The side wall was folded up against the back wall, with the task in mind to align the lock-features. (3) The actuator was folded up, and aligned with the adjoining back wall corner. (4) The corner locks had to be clasped by pushing against them under a proper angle.

Figure 8 and **Figure 9** show the top view of the cell, before and nearly after finishing bending, with the actuator close to its final position.
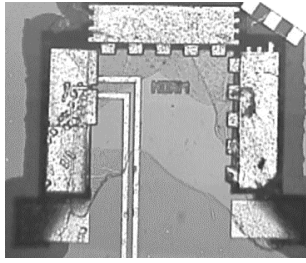
Figure 8. Top view of whole cell before bending up.
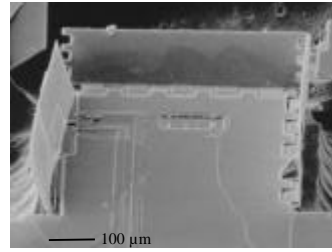

Figure 9. SEM top view of folded-up cell.

5. RESULTS AND OUTLOOK

In this section, we point out the main results as well as the major problems that were observed during the project.

5.1. Problems and Suggestions for Solutions

'Dirty' PITs

An essential prerequisite for a uniform etch of the walls was the cleanliness of the holes that opened up the silicon substrate, the so-called PIT-layer. Unfortunately, various remnants were accumulated in these holes, such as polysilicon, oxide, and metal. A large amount of efforts was necessary to treat every test sample individually to clean off these remnants without destroying the structures themselves. Remainders of such layers that connected to the substrate had to be broken off manually while erecting the walls.

A similar problem came from aluminum that was not etched away entirely from corners of the lock structures and between the hinges. The metal had to be removed using aluminum etchant that affected the wall surfaces in the same way as it dissolved the unwanted material. This resulted in somewhat thinner and therefore weaker walls.

The next design will use improved and safer design rules as well as a different process in order to obtain cleaner results.

Shorts

Even worse was the effect of the surplus metal on the electrical circuitry. Essentially all samples showed shorts that could only be removed by etching away so much aluminum that they were no longer usable for the purpose of fixturing. We suspect that fabrication flaws and the lack of official design rules are responsible for this problem, since the layout was checked carefully and did not give any indication for this behavior. As for the 'dirt' problem, the next design generation will take improved and safer design rules into account in order to avoid these problems.

Bad Surface Quality

Many of the walls showed smaller or larger indents, scratches, and overall a rather bumpy surface. Although the walls are (for microscales) rather large, these flaws were in some cases so severe that the sample could not be used. The yield was reduced by about one third. At the same time, the friction coefficient might decrease beyond the calculated limit, so that another process with improved surface quality should be chosen for the next run.

Remaining Etch Holes

Due to the necessity of underetching the walls, wide and deep holes remained in the silicon substrate. For the prototype, this might be acceptable, but in general, these holes that act as traps for parts to be fixtured, so that other possibilities to release the walls should be explored. These could include manual filling up the holes with photoresist, or usage of a POLY-1 sacrificial layer.

5.2. Future Work

Future work will include an improved and enhanced design, its fabrication and an evaluation of the actuator properties, as well as combination with a sensing mechanism (optical, capacitive, mechanical,...). In the long term, alternative, 'self-erecting' designs (e.g., using scratch drives or microengines [25]) and techniques avoiding the deep etch holes (by using a sacrificial layer) have to be explored.

5.3. Summary

We built and assembled a microfixture fabricated in a standard CMOS process, using aluminum hinges and a XeF_2-release etch. We introduced process-specific features (such as curl in CMOS) to enhance stability and yield, and calculated the stability and strength of the cell.

Sufficient mechanical stability was proven by calculating various scenarios using simple models, in which mechanical stability for the cell could be proved. These models take friction and external forces as well as resonance into account. Practical evidence was given by folding up the cell walls without damage.

Sufficient electrical and thermal properties were shown using established formulas. Thermal and electrical properties were estimated to be sufficient for the task of opening the actuator while optimizing the efficiency.

REFERENCES

1. M. B. Cohn, K.-F. Böhringer, J. M. Novorolski, A. Singh, C. G. Keller, K.. Goldberg, and R. T. Howe, "Microassembly Technologies for MEMS," *Proc. SPIE Micromachining and Microfabrication*, Santa Clara, CA, September 21-22, 1998.

2. G. Danuser, I. Pappas, B. Vögeli, W. Zesch, J. Dual, "Manipulation of Microscopic Objects with Nanometer Precision: Potentials and Limitations in Nano-Robot Design," submitted for review to Int. J. On Robotics Research, 1997.

3. A. Sulzmann, J.-M. Bregnet, J. Jacot, "Micromotor assembly using high accurate optical vision feedback for microrobot relative 3d displacement in submicron range," *Transducers – Digest Int. Conf. On Solid-State Sensors and Actuators*, Chicago, IL, June 1997.

4. X. Arreguit, F. A. v. Schalk, F. V. Bauduin, M. Bidivill, E. Raeber, "A CMOS motion detector system for pointing devices," *IEEE J. of Solid-State Circuits*, 30(12), pp. 1916-1921, December 1996.

5. H. Hitakawa, "Advanced parts orientation system has wide application," *Assembly Automation*, 8(3), 1988.

6. K.-F. Böhringer, M. Cohn, K. Goldberg, R.T. Howe, A. Pisano, "Electrostatic self-assembly aided by ultrasonic vibration," *AVS 44th National Symposium*, San Jose, CA, October 1997.

7. F. Chang, R. Yeh, G. Lin, P. Chu, E. Hoffmann, E. Kruglick, and K.S.J. Pister, "Gas-phase silicon micromachining with xenon difluoride," *SPIE's 1995 Symposium on Micromachining and Micro-fabrication,* Austin, USA, Oct. 23-24, 1995.

8. E.G. Hoffmann, "Modular Fixturing," *Manufacturing Technology Press,* Lake Geneva, Wisconsin, 1987.

9. F. Reuleaux, *The Kinematics of Machinery*, Macmilly and Company, 1876. Republished by Dover in 1963.

10. J.K. Salisbury, "Kinematic and Force Analysis of Articulated Hands," *Ph.D. thesis*, MIT 1992. Published in *Robot Hands and the Mechanics of Manipulation*, MIT Press, 1985.

11. R.S. Fearing, "Survey of Sticking Effects for Micro Parts Handling," *IROS*, Pittsburgh, PA, pp. 212-217, 1995.

12. "Introducing the Micromachined Accelerometer Sensor," Analog Devices, Inc., Norwood, MA, 1991.

13. J. B. Sampsell, "The Digital Micromirror Device And Its Application To Projection Displays," *Transducers*, Pacifico, Yokohama, Japan, Jun. 1993, pp. 24-27.

14. M. Parameswaran, H.P. Baltes, Lj. Ristic, A.C. Dhaded, A.M. Robinson, "A new approach for the fabrication of micromechanical structures," *Sensors and Actuators*, vol. 19, p. 289-307, 1989.

15. W. Yun, R.T. Howe, P.R. Gray, "Surface micromachined, digitally force balanced accelerometer with integrated CMOS detection circuitry," *Technical Digest of the 1992 IEEE Solid-State Sensor and Actuator Workshop*, pp. 126-131, June 1992.

16. E.H. Klaassen, R.J. Reay, C. Storment, J. Audy, P. Henry, A.P. Brokaw, G.T.A. Kovacs, "Microma-chined thermally isolated circuits," *Proc. IEEE Solid State Sensor and Actuator Workshop,* pp. 127-131, June 2-6, 1996.

17. K.S.J. Pister, "Hinged polysilicon structures with integrated thin film transistors," *Proc. IEEE Solid State Sensor and Actuator Workshop,* pp. 136-139, June 22-28, 1992.

18. E. Hoffman, B. Warneke, E. Kruglick, J. Weigold, K.S.J. Pister, "3D structures with piezoresistive sensors in standard CMOS," *Proc. IEEE MEMS*, Nagoya, Japan, 1995.

19. G. Lin, K.S.J. Pister, K.P. Roos, "Standard CMOS piezoresistive sensor to quantify heart cell contractile forces," *MEMS 96*, San Diego, CA, pp. 150-155, Feb. 1996.

20. K.-F. Böhringer, K. Goldberg, M. Cohn, R. Howe, and A. Pisano, "Parallel Microassembly Using Electrostatic Force Fields," *IEEE International Conference on Robotics and Automation (ICRA)*, Leuven, Belgium, May 1998.

21. B. Warneke, E. Hoffman, and K.S.J. Pister, "Monolithic Multiple Axis Accelerometer Design in Standard CMOS," *Proc. SPIE 1995 Symposium on Micromachining and Microfabrication*, pp. 95-102, Austin, Texas, October 23-24, 1995.

22. E.J.J. Kruglick, "Aluminum Hinges and Electrostatic Actuators in standard CMOS," *Masters thesis,* University of California at Los Angeles, 1996.

23. A.H. Epstein, S.D. Senturia, et al., "Power MEMS and microengines," *Transducers '97,* vol.2, 1997.

24. B.C. Read, V.M. Bright, J.H. Comtois, "Mechanical and optical characterization of thermal actuators fabricated in a CMOS process," *Proceedings of SPIE – The International Society for Optical Engineering*, vol. 2642, pp. 22-32, October 1995.

25. E. J. Garcia, J. J. Sniegowski, "Surface Micromachined Microengine," *Sensors and Actuators A* 48, pp. 203-214 (1995).